

Article

Detection of the TiO₂ Concentration in the Protective Coatings for the Cultural Heritage by Means of Hyperspectral Data

Antonio Costanzo ^{1,*}, Donatella Ebolese ², Silvestro Antonio Ruffolo ³, Sergio Falcone ¹, Carmelo la Piana ¹, Mauro Francesco La Russa ³, Massimo Musacchio ⁴ and Maria Fabrizia Buongiorno ⁴

¹ National Earthquake Observatory, Istituto Nazionale di Geofisica e Vulcanologia, 87036 Rende, Italy; sergio.falcone@ingv.it (S.F.); carmelo.lapiana@ingv.it (C.I.P.)

² Department of Culture and Society, University of Palermo, 90128 Palermo, Italy; donatellaebolese@gmail.com

³ Department of Biology, Ecology and Earth Sciences, University of Calabria, 87036 Rende, Italy; silvestro.ruffolo@unical.it (S.A.R.); mauro.larussa@unical.it (M.F.L.R.)

⁴ National Earthquake Observatory, Istituto Nazionale di Geofisica e Vulcanologia, 00143 Rome, Italy; massimo.musacchio@ingv.it (M.M.); fabrizia.buongiorno@ingv.it (M.F.B.)

* Correspondence: antonio.costanzo@ingv.it; Tel.: +39-0984-496068

Abstract: Nanotechnology-based materials are currently being tested in the protection of cultural heritage: ethyl silicate or silica nanoparticles dispersed in aqueous colloidal suspensions mixed with titanium dioxide are used as a coating for stone materials. These coatings can play a key role against the degradation of stone materials, due to the deposit of organic matter and other contaminants on the substrate, a phenomenon that produces a greater risk for the monuments in urban areas because of the increasing atmospheric pollution. However, during the application phase, it is important to evaluate the amount of titanium dioxide in the coatings on the substrate, as it can produce a coverage effect on the asset. In this work, we present the hyperspectral data obtained through a field spectroradiometer on samples of different stone materials, which have been prepared in laboratory with an increasing weight percentage of titanium dioxide from 0 to 8 wt%. The data showed spectral signatures dependent on the content of titanium dioxide in the wavelength range 350–400 nm. Afterwards, blind tests were performed on other samples in order to evaluate the reliability of these measurements in detecting the unknown weight percentage of titanium dioxide. Moreover, an investigation was also performed on a test application of nanoparticle coatings on a stone statue located in a coastal town in Calabria (southern Italy). The results showed that the surveys can be useful for verifying the phase of application of the coating on cultural heritage structures; however, they could also be used to check the state of the coated stone directly exposed over time to atmospheric, biological and chemical agents.

Keywords: protective coatings; nanoparticle films; titanium dioxide; stone surface conservation; spectroradiometric data; hyperspectral signatures; cultural heritage protection



Citation: Costanzo, A.; Ebolese, D.; Ruffolo, S.A.; Falcone, S.; la Piana, C.; La Russa, M.F.; Musacchio, M.; Buongiorno, M.F. Detection of the TiO₂ Concentration in the Protective Coatings for the Cultural Heritage by Means of Hyperspectral Data. *Sustainability* **2021**, *13*, 92. <https://dx.doi.org/10.3390/su13010092>

Received: 25 November 2020

Accepted: 21 December 2020

Published: 24 December 2020

Publisher's Note: MDPI stays neutral with regard to jurisdictional claims in published maps and institutional affiliations.



Copyright: © 2020 by the authors. Licensee MDPI, Basel, Switzerland. This article is an open access article distributed under the terms and conditions of the Creative Commons Attribution (CC BY) license (<https://creativecommons.org/licenses/by/4.0/>).

1. Introduction

Preserving memories means taking care of our past in looking to our future. Conserving the identity, in its huge variety, of our world cultural heritage will ensure solid roots are maintained for future generations. Cultural heritage encompasses a vast area and includes different types of historical and artistic goods, tangibles and intangibles. Each one of these requires a particular preservation procedure, often customized in relation to the environment with a holistic view (e.g., [1]).

There are many components of the urban landscapes which are often subjected to negative effects due to interaction with the surrounding environment. In these landscapes, historical buildings and monuments, often built in natural and artificial stone materials, are among the more exposed elements [2–4]. In fact, pollution and high concentrations of fine particulates, typical of the urban environment, play a role in accelerating the deterioration

process of outdoor surfaces (such as the façades of buildings, architectural elements and sculptures). A challenging issue for conservation is to face the deterioration of stone materials used in the artistic/architectural field (lime-based murals, limestone [5]).

The main causes of decay can be attributed to air pollution, soluble salts and biodeterioration; much research is available in the literature concerning the investigation of their mechanisms of action [6–13]. Identification of the basic principles for a correct conservation treatment is fundamental in defining appropriate actions and for the selection of materials and procedures, also taking into account the intrinsic stone properties, the degradation mechanisms and the environmental factors.

In this framework, the consolidation and protection of cultural heritage can count on innovative materials provided by nanotechnologies: consolidating products and/or protective treatments are improved by being implemented together with nanoproducts with self-cleaning and biocidal characteristics, such as titanium dioxide (TiO₂). These treatments are already a common practice in preservation of stone surfaces. The nanometric TiO₂ is considered a promising photocatalytic material because it has showed ability to catalyze the complete degradation of many organic contaminants and environmental pollutants, leading to a self-cleaning and antimicrobial effect [5,14–16].

As part of a broader contribution to the analysis of the photocatalytic properties of titanium dioxide (TiO₂) through a multi-analytical approach, and also considering that this nanoproduct can represent an environmental friendly alternative in the disinfection of stone surfaces, the article presents a procedure to support the control of TiO₂ concentration in the coatings by field spectroradiometric surveys. In Section 2 the preparation of the samples and spectroradiometric survey method are illustrated. The main results and their interpretation are discussed in Section 3. A recap of the work and some concluding remarks are reported in Section 4.

2. Materials and Methods

In the literature there are several researches aimed at the characterization of TiO₂-based coatings applied on different support stone materials (e.g., [14,17–20]); in particular, they analyze the biocidal and photodegradation efficiency, the color variations and hydrophobic properties, the distribution of TiO₂ in depth, the acid resistance and the morphological characterization. In addition, other tests were performed to study the long-term behavior of the coating subjected to artificial ageing [21]. In this work, we present a method to analyze the state of the coating through quick and contactless measurements performed directly on the application stone, so as to permit the inspection of different parts of the same object and/or on widespread cultural heritage assets. In particular, in a first phase the correlations were obtained by analyzing the percentage concentrations by weight of TiO₂ in the coatings, as they were provided by the production laboratory, and the hyperspectral data obtained once the same coatings were applied on stone samples. Subsequently, these correlations were used to evaluate the correspondence between the findings by the field measurements and the laboratory information on applications of coatings with an unknown TiO₂ concentration.

2.1. Sample Preparation in Laboratory

Marble and travertine samples were treated with formulations containing Nano Estel[®] [22], TEOS (tetraethyl orthosilicate) [23,24] and Aeroxide[®] TiO₂ P25 titanium dioxide [25].

Nano Estel is a colloid formulation wherein the particles of SiO₂ are dispersed in a water-based solution. The dispersed nanoparticles have a diameter not greater than 20 nm. The particles connect to each other, after the evaporation of the water, to produce a silica gel with a consolidating effect, thanks to the bridges generated between the detached particles of the support material.

Aeroxide TiO₂ P25 consists of particles having mean diameter of approximately 21 nm with a high photoactivity. In the presented experiment, Nano Estel and TEOS were

diluted to 3% with deionized water and, after that, mixed with different weight percentage concentrations of TiO_2 (from 0 to 8 wt%). These coatings, with increasing concentrations of nanoproductions, were applied on marble (Figure 1) and travertine samples.



Figure 1. Laboratory marble samples with coatings blended with solutions of increased weight percentage concentration of titanium dioxide.

Once the coatings had been applied, after 30 days for drying, surface spectral measurements were performed on samples of marble or travertine covered by Nano Estel or TEOS, respectively. In particular, for each stone material and coating the hyperspectral signatures were acquired on 7 samples: 1 of untreated stone, 1 of stone with coating (Nano Estel or TEOS) without TiO_2 , and 5 with coating blended with an increasing TiO_2 weight percentage (0.5, 1, 2, 4 and 8 wt%).

2.2. Spectroradiometric Surveys

Measurements of solar reflected radiance were carried out with FieldSpec pro portable spectroradiometer (ASD Inc., Longmont, CO, USA) [26]. The instrumentation was equipped with three different spectrometers covering the 350–2500 nm spectral range: the first detector worked in the VNIR range (350–1000 nm), and the other two in the SWIR region (1001–1800 and 1801–2500 nm, respectively). These sensors are characterized by spectral resolution of 3 nm at 700 nm and 10 nm at 1400–2100 nm; spectral sampling of 1.4 and 1.1 nm in the ranges 350–1000 nm and 1001–2500 nm, respectively; and wavelength accuracy 0.5 nm. All details about the technical specifications of the instrumentation are available in [26].

The surveys were performed directly using bare fiber optic cable linked to the instrument and mounted on the pistol (i.e., without the use of specific lenses); a field of view of 25° corresponds to this configuration. The fore optic was pointed toward the target in opposite direction to the incidence of the solar rays to form an angle of about 90° , trying to keep constant the distance between the fore optic and the objects. Moreover, the distance between fiber fore optic and target was kept constant as much as possible. For each measurement, 25 spectral signatures were collected and the mean values were calculated, directly, by the acquisition software. Furthermore, for each sample 10 measurement points were performed in order to take into account variability of the local conditions due to the coating application and the base stone.

3. Results and Discussion

As already shown by Costanzo et al. [27], for marble coated with Nano Estel, we found appreciable differences among the reflectance values in the ultraviolet range (350–

400 nm) of the electromagnetic spectrum as a function of the amount of Aeroxide TiO₂ P25 in the coating, these changes were common to all the analyzed combinations between the stone base materials and the type of TiO₂ coatings (cf. Figures 2–5). This behavior is strongly linked to the weight percentage of titanium dioxide added in the coating; in fact, by analyzing the spectral signature of the titanium dioxide provided in the ASTER spectral library [28] and graphically represented in Figure 6, it can be noted there was a high slope in the wavelength range between 350 and 400 nm, with a strong decrease of the reflectance moving towards the ultraviolet range.

The comparison between the spectral signatures of the laboratory samples shows some differences between the untreated material and the stone coated with the materials prepared without TiO₂; however, the differences become even more appreciable with the increase of TiO₂ up to 4 wt%. Instead, beyond this last value, the spectral shapes seemed more similar although much larger amounts of TiO₂ were blended into the coating.

To obtain a representative pattern as a function of the TiO₂ variation, the spectral signatures in the bands between 350 and 400 nm were compared with that obtained for the untreated stone through the spectral angle mapper (SAM) technique [29]. In fact, this technique allows calculation of the coefficient *SA*, representing the angular difference (in radians) between a given spectrum and the reference one, through the follow equation:

$$SA = \cos^{-1} \left(\frac{\sum_{i=1}^{nb} t_i r_i}{\sqrt{\sum_{i=1}^{nb} t_i^2} \sqrt{\sum_{i=1}^{nb} r_i^2}} \right)$$

Here, *nb* is the number of the spectral bands; *t_i* and *r_i* are the reflectance values for the spectral band *i* in the spectrum to be analyzed and the reference one, respectively. The pair of spectra is treated as a vector in *nb*-space, allowing us to calculate similarity between them. The zero value of the *SA* coefficient represents the maximum similarity (i.e., spectral shapes are identical), while the increasing values define a decreasing similarity.

It is worth noting that higher *SA* values are expected for larger concentrations of TiO₂, because of the increasing differences in the ultraviolet range between spectral shapes (see Figures 2–5) compared to untreated material.

The similarities have been calculated in terms of *SA* for each material and each coating (Figure 7). The graphs in the figure show the trends as a function of the TiO₂ weight: the values increase significantly up to 4 wt%; the difference, on the other hand, is practically negligible when comparing those with 4 and 8 wt%. Therefore, the correlations are able to indicate the amount of TiO₂ when it is less than 4 wt%, while they do not allow discrimination of larger quantities with reliability.

Moreover, the *SA* values obtained for the different stone materials with the same coating appear comparable; therefore, only a relationship was calculated for each coating material (cf. Figure 8). In addition, some blind tests were performed to evaluate the capability to detect the unknown weight percentage concentrations of TiO₂ wt%. In particular, the correlations were used to evaluate the weight percentage concentration of TiO₂ of 12 samples: 6 of marble (cf. green triangles in Figure 8) and 6 of travertine (cf. red triangles in Figure 8). The concentrations determined by means of spectroradiometric measurements, after the application of the coating materials by brushing on the stones, were compared to those of the coating production provided by the laboratory (Table 1): the differences seem almost always contained; in fact, the absolute values are equal to or less than 0.5. Only one of the tests showed a significant deviation. It is worth pointing out that the differences can be related not only to the error introduced by correlations, but also due to the actual concentration of TiO₂ in the coating placed on the stone following the application method.

The correlations were also used to evaluate the concentration of TiO₂ in the coatings applied as a test at the foot of the statue, called “Angelo Tutelare”, exhibited in a square of the coastal urban center of Reggio Calabria city (Calabria, Southern Italy) (cf. 3D reconstruction by terrestrial laser scanning in Figure 9). Petrographic survey indicates that

the statue was made in Greek marble, probably with waste materials from the ruins of a temple in the Magna Graecia city [30]. The spectral signatures were acquired before and after applying Nano Estel and TEOS coatings on small parts of the basement near the two feet (Figure 9).

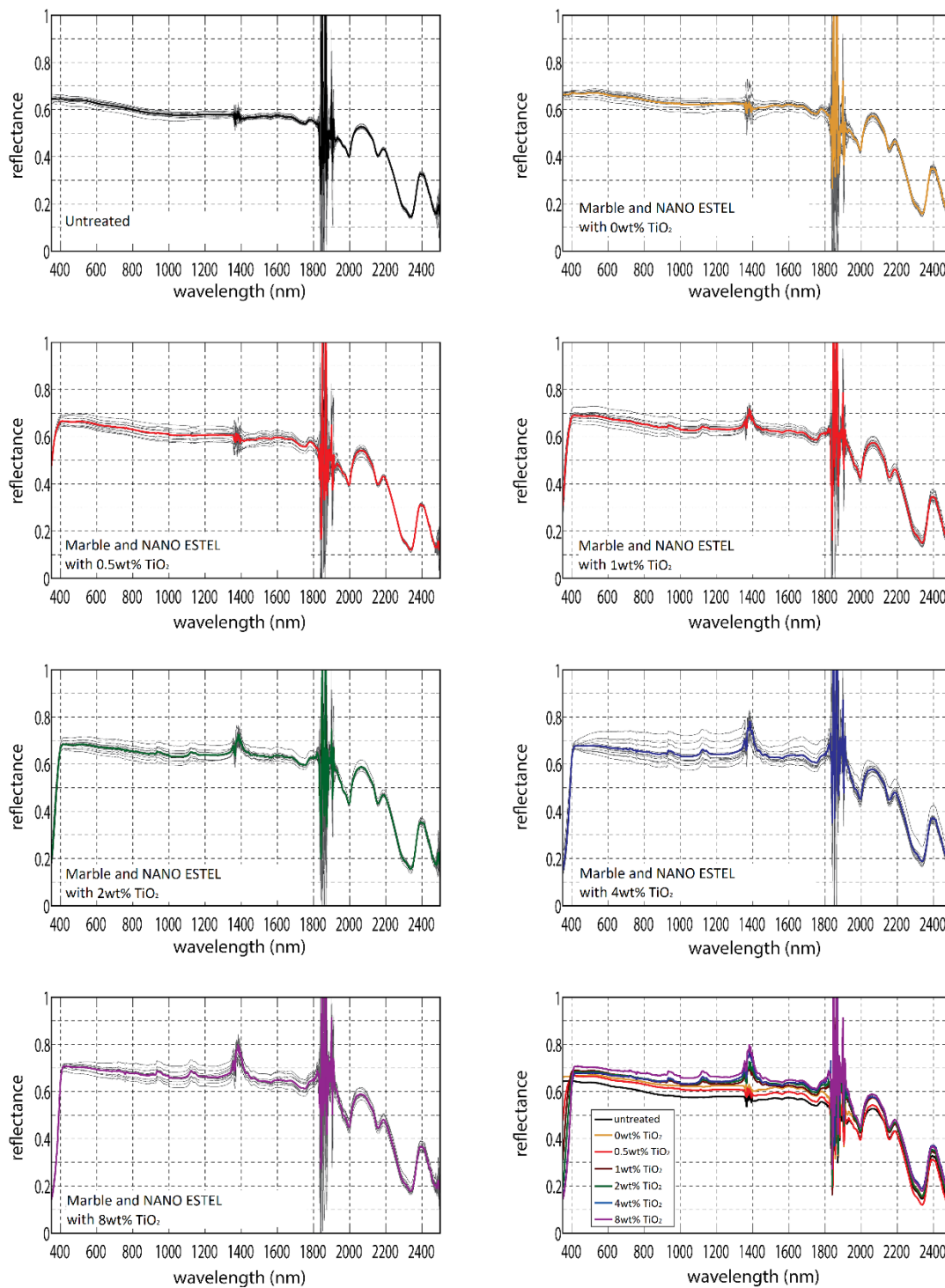


Figure 2. Spectral signatures obtained by spectroradiometric survey of the surface of marble samples prepared in laboratory with Nano Estel coatings blended with different weight percentage concentrations of titanium dioxide (TiO₂). In each graph, the gray curves represent the spectral data for different measurement areas on the same sample, each of which is the average calculated over 25 measurements on the same area during the acquisition phase, whereas the colored curve is the mean spectral signature. The overlap of the different signatures (bottom right graph) shows the effect due to the increasing wt% of TiO₂.

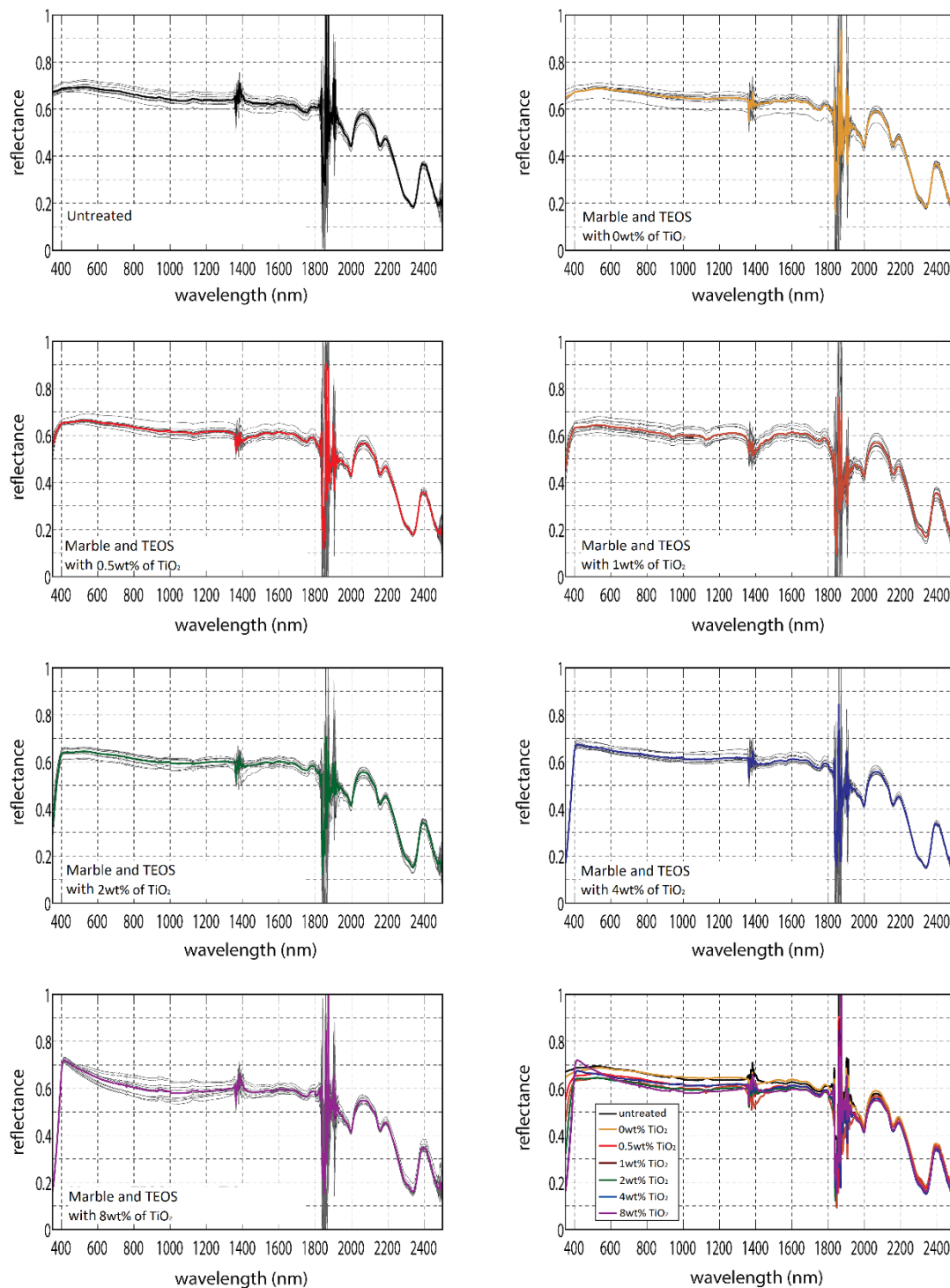


Figure 3. Spectral signatures obtained by spectroradiometric survey of the surface of marble samples prepared in laboratory with TEOS coatings blended with different weight percentage concentrations of titanium dioxide (TiO_2). In each graph, the gray curves represent the spectral data for different measurement areas on the same sample, each of which is the average calculated over 25 measurements on the same area during the acquisition phase, whereas the colored curve is the mean spectral signature. The overlap of the different signatures (bottom right graph) shows the effect due to the increasing wt% of TiO_2 .

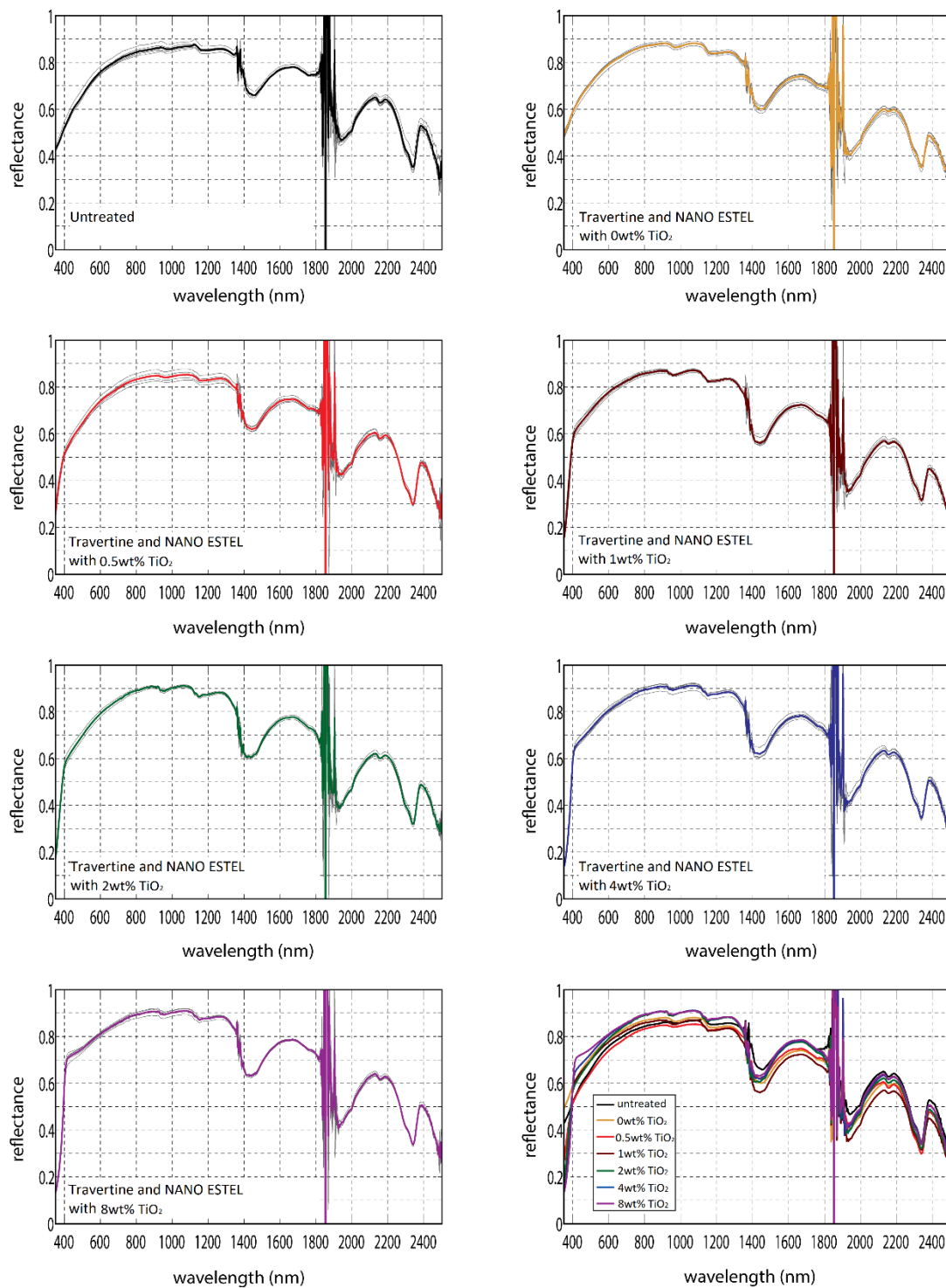


Figure 4. Spectral signatures obtained by spectroradiometric survey of the surface of travertine samples prepared in laboratory with Nano Estel coatings blended with different weight percentage concentrations of titanium dioxide (TiO_2). In each graph, the gray curves represent the spectral data for different measurement areas on the same sample, each of which is the average calculated over 25 measurements on the same area during the acquisition phase, whereas the colored curve is the mean spectral signature. The overlap of the different signatures (bottom right graph) shows the effect due to the increasing wt% of TiO_2 .

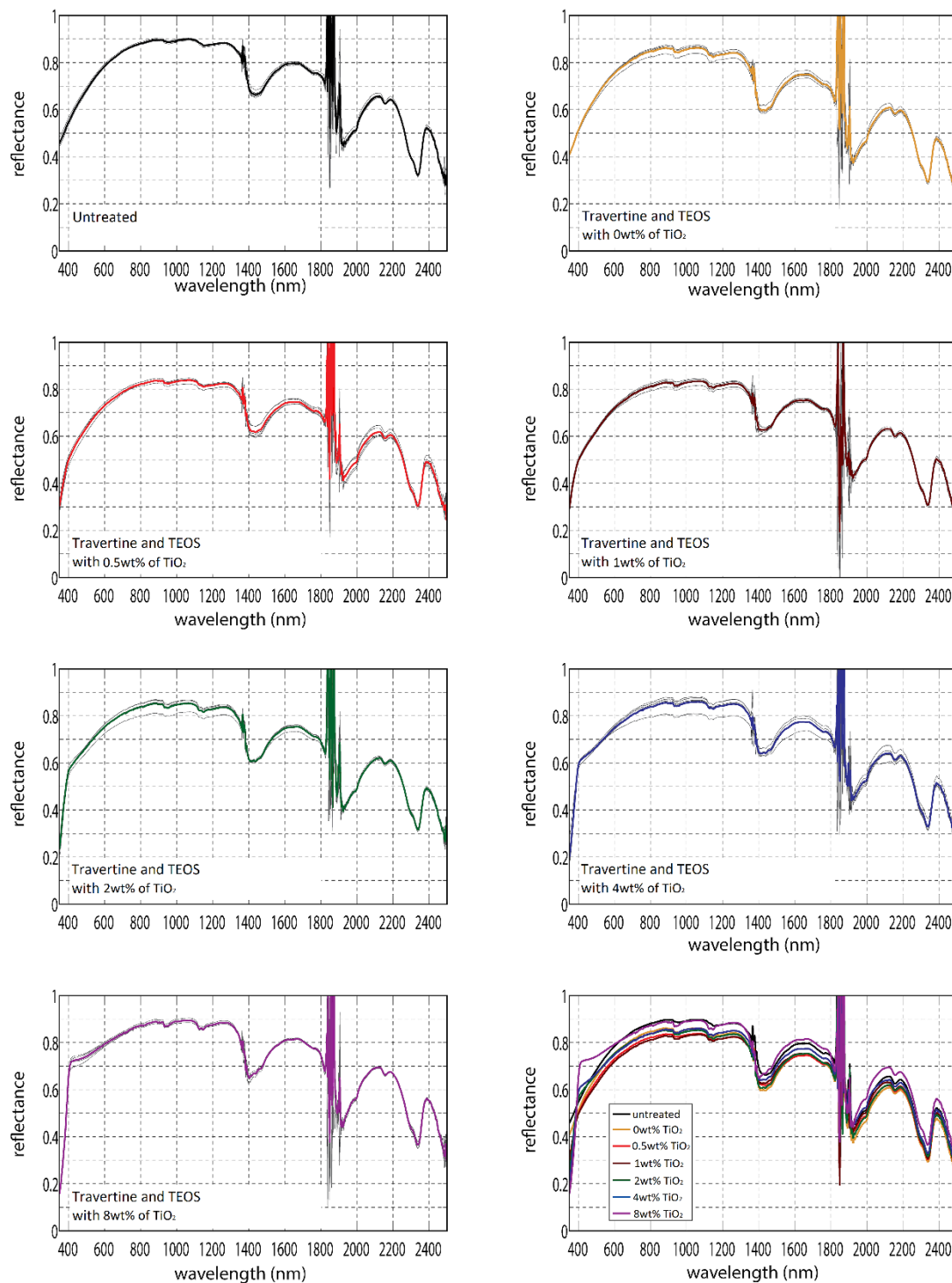


Figure 5. Spectral signatures obtained by spectroradiometric survey of the surface of travertine samples prepared in laboratory with TEOS coatings blended with different weight percentage concentrations of titanium dioxide (TiO_2). In each graph, the gray curves represent the spectral data for different measurement areas on the same sample, each of which is the average calculated over 25 measurements on the same area during the acquisition phase, whereas the colored curve is the mean spectral signature. The overlap of the different signatures (bottom right graph) shows the effect due to the increasing wt% of TiO_2 .

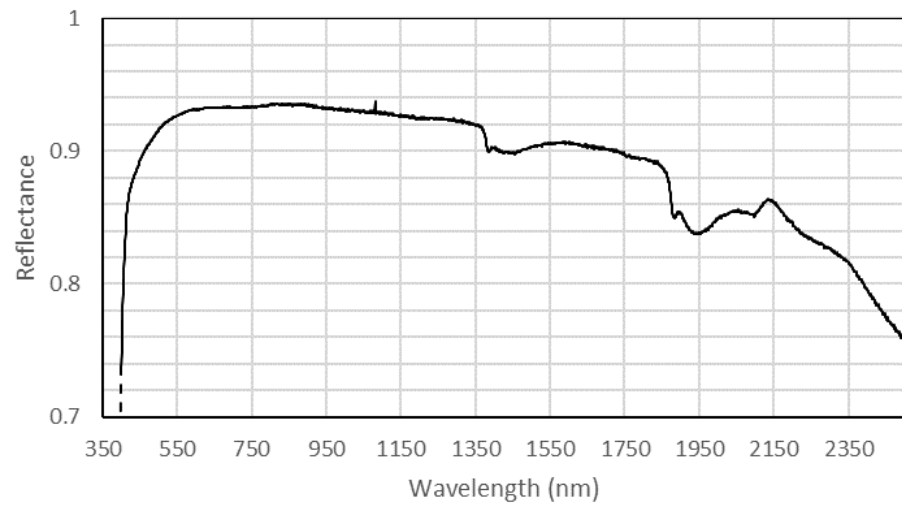


Figure 6. Spectral signature of the titanium dioxide (ASTER spectral library [28]).

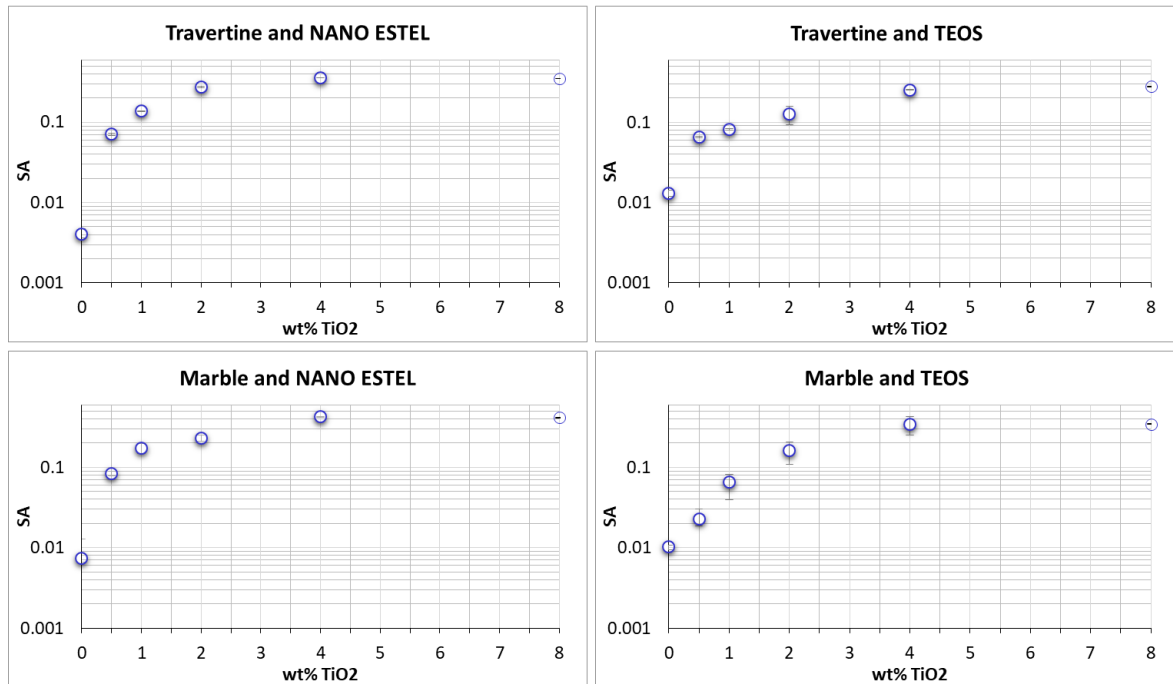


Figure 7. Spectral angle coefficient calculated from the spectral shapes obtained for the different stone materials and coatings (cf. Figures 2–5), using the untreated stones as reference. The coefficients are a function of the amounts of TiO₂ in the coatings. SA values are reported for travertine and marble coated with Nano Estel or TEOS.

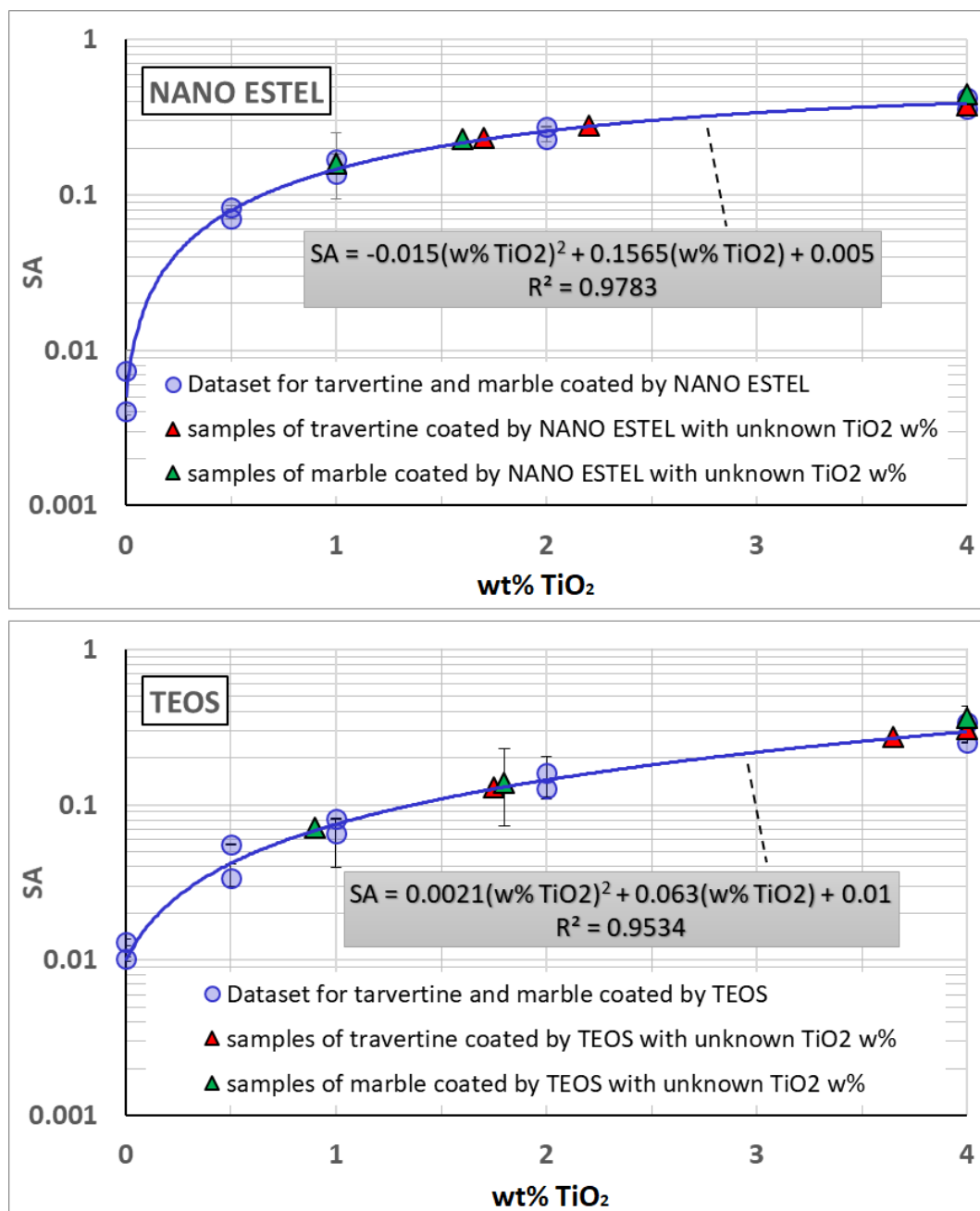
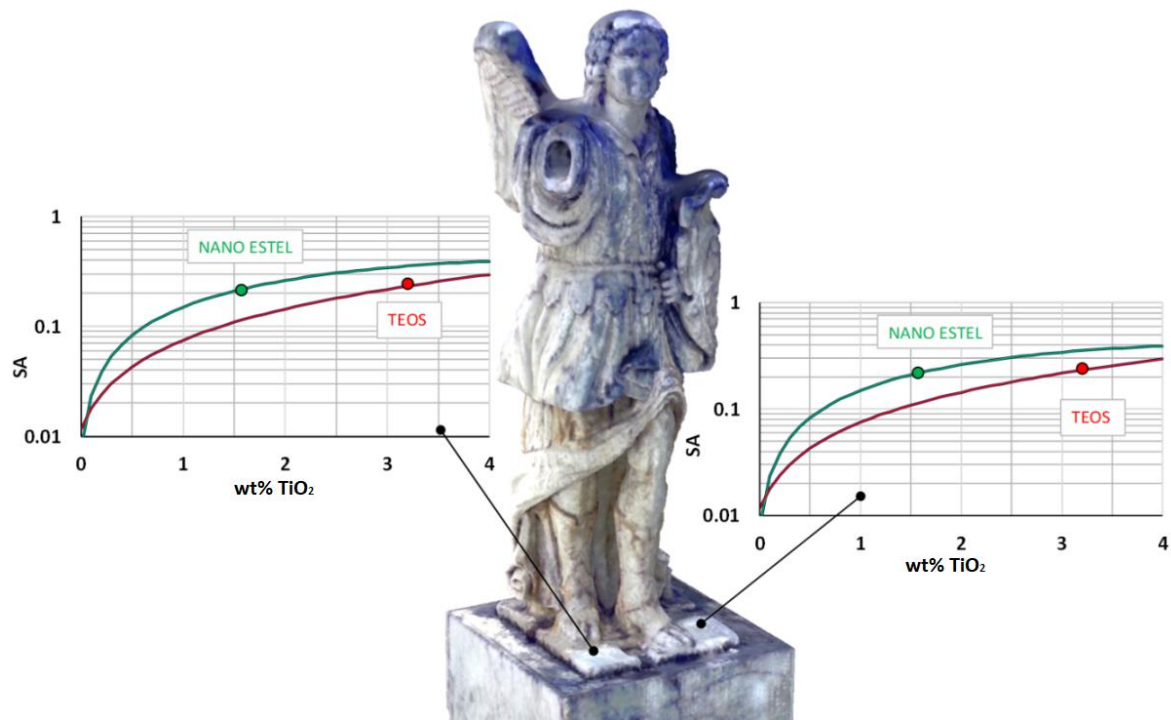


Figure 8. Correlations between spectral angle and TiO₂ wt% combining data for marble and travertine with the same coatings: Nano Estel (blue circles on upper graph) and TEOS (blue circles on lower graph). In addition, the data obtained on samples with unknown TiO₂ wt% are also reported on the curves in order to evaluate their values (red triangles for travertine and green triangles for marble).

Table 1. Differences between TiO₂ weight percentage concentrations in the coatings obtained by spectroradiometric measures and laboratory.

	Stone	Coating	TiO ₂ wt% by Laboratory	TiO ₂ wt% by Hyperspectral Survey	Difference of TiO ₂ wt%
1	Travertine	Nano Estel	10	≥4	-
2	Travertine	Nano Estel	2	1.7	0.3
3	Travertine	Nano Estel	4	2.2	1.8
4	Travertine	TEOS	10	≥4	-
5	Travertine	TEOS	2	1.8	0.2
6	Travertine	TEOS	4	3.7	0.3
7	Marble	Nano Estel	10	≥4	-
8	Marble	Nano Estel	0.5	1.0	−0.5
9	Marble	Nano Estel	2	1.6	0.4
10	Marble	TEOS	10	≥4	-
11	Marble	TEOS	0.5	0.9	−0.4
12	Marble	TEOS	2	1.8	0.2

**Figure 9.** Applications of TiO₂-coatings Nano Estel and TEOS on small parts of the “Angelo Tutelare” statue located in the coastal urban environment of Reggio Calabria city. The 3D reconstruction of the statue was performed by terrestrial laser scanning. The graphs show the values of TiO₂ wt% in the coatings obtained through the correlations of Figure 8.

By using the previous correlations, the TiO₂ wt% was evaluated in the graphs in Figure 3. Values were obtained of 1.7 wt% for the Nano Estel and 3.2 wt% for TEOS, which are in line with those from the laboratory of 2 and 3 wt%, respectively. Equal values were obtained by the hyperspectral measurements carried out on the two applications performed for each coating.

4. Conclusions

Many structures of cultural heritage significance, especially those located in urban environments, are often exposed to negative effects due to high pollution and concentrations of fine particulate. In particular, the objects and elements in stone material suffer an

acceleration of the degradation processes because of these phenomena. However, coatings containing nanoproducts such as titanium dioxide (TiO_2), today represent a powerful tool to mitigate stone degradation in a sustainable way. The durability of such coatings is also related to the persistence of the nanoproduct on the surface itself. This work has dealt with the detection and the monitoring of the TiO_2 concentration blended into the protective coatings applied on stone materials. In particular, hyperspectral data were analyzed in order to identify an indicator of the amount of TiO_2 . The measurements carried out by field spectroradiometric sensors allowed us to obtain reflectance values for different stones and coverage materials. In particular, data analysis was performed for coatings based on Nano Estel and TEOS with addition of different weight percentage concentrations of Aeroxide TiO_2 P25. The spectral signatures of the coated stone depending on the amount of titanium dioxide (TiO_2) blended into the coating, with the effect on the wavelength ranging between 350 and 400 nm. Nevertheless, the increasing amount of TiO_2 had gradually less effect; results were practically negligible for values greater than 4 wt%. The data analysis allowed us to calculate a relationship for each coating regardless of the base material. Afterwards, blind tests were performed on samples of marble or travertine covered with the two coatings; the tests seemed able to identify the weight percentage concentration of TiO_2 with a good reliability. Furthermore, tests were performed on some applications carried out on a statue placed in a coastal urban environment. Even in this case the correlations matched with good approximation those provided by the laboratory. Further surveys will be performed on coating applications to protect architectural elements and sculpture exposed to weather, biological and chemical agents, with the purpose being to evaluate the state of the coating over time.

Author Contributions: Conceptualization, A.C., M.F.L.R., and M.M.; methodology, A.C.; formal analysis, A.C.; investigation, A.C., C.I.P., D.E., S.A.R., and S.F.; data curation, A.C., D.E., and S.A.R.; writing—original draft preparation, A.C., M.M., and S.A.R.; funding acquisition, M.F.B.; writing—review and editing, A.C. supported by all authors. All authors have read and agreed to the published version of the manuscript.

Funding: Activities of the research were partially funded by Project MIUR 2020-2029 Pianeta Dinamico: Geoscienze per la comprensione dei meccanismi di funzionamento della Terra e dei conseguenti rischi naturali—Working Earth: geosciences and understanding of the earth dynamics and natural hazards” (CUP D53J19000170001).

Institutional Review Board Statement: Not applicable.

Informed Consent Statement: Not applicable.

Data Availability Statement: The data presented in this study are available on request from the corresponding author.

Acknowledgments: The authors thank the staff members who supported the processes necessary to carry out the laboratory and survey activities. In addition, they thank the three anonymous reviewers for their fruitful suggestions to improve the article.

Conflicts of Interest: The authors declare no conflict of interest. The funders had no role in the design of the study; in the collection, analyses, or interpretation of data; in the writing of the manuscript, or in the decision to publish the results.

References

1. Bazazzadeh, H.; Nadolny, A.; Attarian, K.; Najar, B.S.A.; Safaei, S.S.H. Promoting Sustainable Development of Cultural Assets by Improving Users' Perception through Space Configuration; Case Study: The Industrial Heritage Site. *Sustainability* **2020**, *12*, 5109. [[CrossRef](#)]
2. Jackson, M.D.; Marra, F.; Hay, R.L.; Cawood, C.; Winkler, E.M. The judicious selection and preservation of tuff and travertine building stone in ancient Rome. *Archaeometry* **2005**, *47*, 485–510. [[CrossRef](#)]
3. Bourges, A.; Fehr, K.T.; Simon, S.; Snethlage, R. Correlation between the micro-structure and the macroscopic behaviour of sandstones. *Restor. Build. Monum.* **2008**, *14*, 157–166. [[CrossRef](#)]
4. Ruggiero, L.; Fidanza, M.R.; Iorio, M.; Tortora, L.; Caneva, G.; Ricci, M.A.; Sodo, A. Synthesis and Characterization of TEOS Coating Added with Innovative Antifouling Silica Nanocontainers and TiO_2 Nanoparticle. *Front. Mater.* **2020**, *7*, 185. [[CrossRef](#)]

5. La Russa, M.F.; Rovella, N.; de Buergo, M.A.; Belfiore, C.M.; Pezzino, A.; Crisci, G.M.; Ruffolo, S.A. Nano-TiO₂ coatings for cultural heritage protection: The role of the binder on hydrophobic and self-cleaning efficacy. *Prog. Org. Coat.* **2016**, *91*, 1–8. [[CrossRef](#)]
6. Del Monte, M.; Sabbioni, C.; Vittori, O. Airborne carbon particles and marble deterioration. *Atmos. Environ.* **1981**, *15*, 645–665. [[CrossRef](#)]
7. Amoroso, G.G.; Fassina, V. *Stone Decay and Conservation: Atmospheric Pollution, Cleaning Consolidation and Protection*; Elsevier: Amsterdam, The Netherlands, 1983.
8. Diakumaku, E.; Gorbushina, A.A.; Krumbein, W.E.; Panina, L.; Soukharjevski, S. Black fungi in marble and limestones—An aesthetical, chemical and physical problem for the conservation of monuments. *Sci. Total Environ.* **1995**, *167*, 295–304. [[CrossRef](#)]
9. Primerano, P.; Marino, G.; Di Pasquale, S.; Mavilia, L.; Corigliano, F. Possible alteration of monuments caused by particles emitted into the atmosphere carrying strong primary acidity. *Atmos. Environ.* **2000**, *34*, 3889–3896. [[CrossRef](#)]
10. Ruffolo, S.A.; La Russa, M.F.; Ricca, M.; Belfiore, C.M.; Macchia, A.; Comite, V.; Pezzino, A.; Crisci, G.M. New insights on the consolidation of salt weathered limestone: The case study of Modica stone. *Bull. Eng. Geol. Environ.* **2017**, *76*, 11–20. [[CrossRef](#)]
11. Cardell, C.; Delalieux, F.; Roumpopoulos, K.; Moropoulou, A.; Auger, F.; Van Grieken, R. Salt-induced decay in calcareous stone monuments and buildings in a marine environment in SW France. *Constr. Build. Mater.* **2003**, *17*, 165–179. [[CrossRef](#)]
12. McNamara, C.J.; Mitchell, R. Microbial deterioration of historic stone. *Front. Ecol. Environ.* **2005**, *3*, 445–451. [[CrossRef](#)]
13. Scheerer, S.; Ortega-Morales, O.; Gaylarde, C. Microbial deterioration of stone monuments—An updated overview. *Adv. Appl. Microbiol.* **2009**, *66*, 97–139. [[CrossRef](#)] [[PubMed](#)]
14. La Russa, M.F.; Ruffolo, S.A.; Rovella, N.; Belfiore, C.M.; Palermo, A.M.; Guzzi, M.T.; Crisci, G.M. Multifunctional TiO₂ coatings for Cultural Heritage. *Prog. Org. Coat.* **2012**, *74*, 186–191. [[CrossRef](#)]
15. Ruffolo, S.A.; De Leo, F.; Ricca, M.; Arcudi, A.; Silvestri, C.; Bruno, L.; Urzi, C.; La Russa, M.F. Medium-term in situ experiment by using organic biocides and titanium dioxide for the mitigation of microbial colonization on stone surfaces. *Int. Biodeterior. Biodegrad.* **2017**, *123*, 17–26. [[CrossRef](#)]
16. Munafò, P.; Goffredo, G.B.; Quagliarini, E. TiO₂-based nanocoatings for preserving architectural stone surfaces: An overview. *Constr. Build. Mater.* **2015**, *84*, 201–218. [[CrossRef](#)]
17. La Russa, M.F.; Barone, G.; Belfiore, C.M.; Mazzoleni, P.; Pezzino, A. Application of protective products to “Noto” calcarenite (south-eastern Sicily): A case study for the conservation of stone materials. *Environ. Earth Sci.* **2011**, *62*, 1263–1272. [[CrossRef](#)]
18. Shu, H.; Yang, M.; Liu, Q.; Luo, M. Study of TiO₂-Modified Sol Coating Material in the Protection of Stone-Built Cultural Heritage. *Coatings* **2020**, *10*, 179. [[CrossRef](#)]
19. Quagliarini, E.; Bondioli, F.; Goffredo, G.B.; Cordoni, C.; Munafò, P. Self-cleaning and de-polluting stone surfaces: TiO₂ nanoparticles for limestone. *Constr. Build. Mater.* **2012**, *37*, 51–57. [[CrossRef](#)]
20. Petronella, F.; Pagliarulo, A.; Truppi, A.; Lettieri, M.; Masieri, M.; Calia, A.; Curri, M.L.; Comparelli, R. TiO₂ Nanocrystal Based Coatings for the Protection of Architectural Stone: The Effect of Solvents in the Spray-Coating Application for a Self-Cleaning Surfaces. *Coatings* **2018**, *8*, 356. [[CrossRef](#)]
21. Roveri, M.; Goidanich, S.; Toniolo, L. Artificial Ageing of Photocatalytic Nanocomposites for the Protection of Natural Stones. *Coatings* **2020**, *10*, 729. [[CrossRef](#)]
22. CTS SRL. NANOESTEL[®]. Available online: <http://www.ctseurope.com/en/scheda-prodotto.php?id=229> (accessed on 8 November 2020).
23. Kim, E.K.; Won, J.; Do, J.-Y.; Kim, S.D.; Kang, Y.S. Effects of silica nanoparticle and GPTMS addition on TEOS-based stone consolidants. *J. Cult. Herit.* **2009**, *10*, 214–221. [[CrossRef](#)]
24. Zárrega, R.; Cervantes, J.; Salazar-Hernandez, C.; Wheeler, G. Effect of the addition of hydroxyl-terminated polydimethylsiloxane to TEOS-based stone consolidants. *J. Cult. Herit.* **2010**, *11*, 138–144. [[CrossRef](#)]
25. EVONIK's AEROXIDE[®] TiO₂ P25. Available online: <https://www.aerosil.com/lpaproductfinder/page/productsbytext/detail.html?pid=1822> (accessed on 8 November 2020).
26. ASD Inc. FieldSpec 4 Standard-Res Spectroradiometer. Available online: <https://www.malvernpanalytical.com/en/products/product-range/asd-range/fieldspec-range> (accessed on 8 November 2020).
27. Costanzo, A.; Ebolese, D.; Falcone, S.; Piana, C.L.; Ruffolo, S.A.; Russa, M.F.L.; Musacchio, M. Hyperspectral Survey Method to Detect the Titanium Dioxide Percentage in the Coatings Applied to the Cultural Heritage. *Proceedings* **2017**, *2*, 120. [[CrossRef](#)]
28. Baldrige, A.M.; Hook, S.J.; Grove, C.I.; Rivera, G. The ASTER spectral library version 2.0. *Remote Sens. Environ.* **2009**, *113*, 711–715. [[CrossRef](#)]
29. Yuhas, R.H.; Goetz, A.F.H.; Boardman, J.W. Discrimination among Semi-Arid Landscape Endmembers Using the Spectral Angle Mapper (SAM) Algorithm. In *AVIRIS Workshop, Proceedings of the Summaries of the 3rd Annual JPL Airborne Geoscience Workshop, Washington, DC, USA, 1–15 June 1992*; JPL Publication: Washington, DC, USA, 1992; Volume I, pp. 147–149.
30. Sorrenti, M.T. *L'Angelo Tutelare di Reggio Calabria: Lettura Critica e Restauro [The Angelo Tutelare of Reggio Calabria: Critical Reading and Restoration]*; Valtieri, S., Ed.; Quaderni del Dipartimento Patrimonio Architettonico e Urbanistico: Rome, Italy, 1999; pp. 16–18.